



Collective dynamics of dipolar self-propelled particles

N. Vanesse, E. Opsomer, G. Lumay, and N. Vandewalle 
 GRASP, Institute of Physics B5a, University of Liège, 4000 Liège, Belgium

 (Received 17 May 2023; accepted 13 June 2023; published 18 August 2023)

We present a numerical study of the collective behavior of self-propelled particles for which dipolar interactions are considered. These are obtained by introducing pointlike magnetic dipoles in the particles. Various dynamical regimes are found depending on three major parameters: the density of particles, the ratio Γ defined as the competition between kinetic energy and potential magnetic energy, as well as the orientation of the magnetic dipoles inherent to the particles. Patterns such as chains, vortices, flocks, and strips have been obtained.

DOI: [10.1103/PhysRevE.108.024608](https://doi.org/10.1103/PhysRevE.108.024608)

I. INTRODUCTION

Active matter is composed of basic elements that consume energy from their environment and convert it in order to act by themselves, providing function or motion. Therefore, active systems are intrinsically out of equilibrium. A large class of active systems is composed of self-propelled particles. Paradigmatic examples are fish schools and shoals [1–4], bird flocks [5–8], artificial self-propelled colloidal particles [9–11], and swarms of robots [12,13]. These systems can be classified into two main categories: living organisms and inert particles. However, for cost or maintenance reasons, such systems can also be studied through numerical simulations [14–19]. In some conditions, these systems could exhibit collective behaviors like swarming, grouping, or vorticing, as well as phase separation [2–4,9,15,20–22].

Since experiments often encounter challenges to control living organisms or be reproduced, model systems like kilobots [23], hexbugs [24], or vibrobots [25] have recently been proposed and studied. In the last case, these particles are typically one centimeter long with flexible inclined legs and their self-propulsion comes from a conversion of energy given by the vertically oscillating support. Depending on how these little legs are positioned around the particles, we may observe linearly moving particles [26–28] or rotating particles [29–31]. When many of them are placed in a closed arena, they show collective dynamics due to their collisions, which represent the only way that these active particles interact with each other. Furthermore, these findings highlight that high densities are required to show large-scale structures in such systems.

Since steric interactions between vibrobots require high densities to trigger collective behaviors, additional local interactions could be added to lowering critical density thresholds. An elegant way to introduce local interactions is to consider dipole-dipole interactions between active particles. The vibrobot counterpart corresponds to magnetic interactions resulting from dipolar magnetic moments inserted in the particles. Recent numerical findings suggested that some patterns like chains and vortices form in those systems, and the vortices seem to be due to wall effects [19].

In this paper, we explore numerically the collective dynamics of an open and dilute system composed of a few dipolar active particles. In particular, we aim to establish a link between the orientation of their dipoles and the resulting patterns. We expect that the dynamics will differ depending on the particle type and density. Figure 1 shows different ways to insert permanent magnets in vibrobots. Like a branching phylogenetic tree, one or two dipoles may be inserted (noted $m1$ and $m2$, respectively). Horizontal dipoles can be orientated along either the major axis a or the minor axis b . Since $m1b_+$ and $m1b_-$ are two versions of the same type of particles, this paper will only focus on three main systems, independently composed of $m2a$, $m1a$, and $m1b$ particles, assuming that label $m1b$ is used for the label $m1b_+$ in the rest of the paper. We expect that the number of inserted dipoles per vibrobot and their orientation may induce different collective behaviors.

II. MODEL

In our model, the self-propelled particles (SPP) have an elliptical shape with aspect ratio $a/b = 1.8$ and their 2D motion was implemented by considering a particle velocity \vec{v} through their components \vec{v}_a and \vec{v}_b along major and minor axes, respectively. The evolution of the velocity of a particle is given by

$$\frac{d}{dt}\vec{v} = \eta(\gamma_a\vec{e}_a + \gamma_b\vec{e}_b) - \beta\vec{v}, \quad (1)$$

where the parameter η is a fitting parameter and β represents damping. Parameters γ_a and γ_b come from the velocity distributions along the base axes of the particle and are randomly drawn at a constant rate.

In addition, a particle tends to reorient its major axis along its velocity, following the equation,

$$\frac{d}{dt}\phi = \xi \sin(\alpha)\text{sgn}(\cos(\alpha)), \quad (2)$$

where ξ is a coupling term and α is the angle between the vector polarization \vec{e}_a and velocity \vec{v} of the particle. More details can be found in the Supplemental Material [32].

The dipolar interactions arise from the classical dipole-dipole potential

$$U(r_{ij}) = \frac{\mu_0}{4\pi} \left[\frac{\vec{\mu}_i \cdot \vec{\mu}_j}{r_{ij}^3} - 3 \frac{(\vec{\mu}_i \cdot \vec{r}_{ij})(\vec{\mu}_j \cdot \vec{r}_{ij})}{r_{ij}^5} \right] \quad (3)$$

providing either attractive or repulsive short-range interactions depending on the relative orientations of the dipoles $\vec{\mu}_i$ and $\vec{\mu}_j$ embedded in two different particles. This potential is known to induce dipole alignments so that particle order is expected.

Systems evolve through interactions and collisions that occur between particles, modifying their motion and orientation. In this way, those interactions were implemented using a discrete element method (DEM) algorithm [33], being a classical numerical approach in the field of granular systems. The forces exerted by the particles on each other were calculated at each time step and were integrated for calculating the new positions and velocities of the particles.

In this paper, we will study the effects of dipolar interactions on the collective dynamics in the system. Therefore, we need to introduce several control parameters. The first one is the number N of SPP that compose the system. The latter were randomly placed in a square arena of length L with periodic boundary conditions. The number N is directly related to the surface fraction covered by particles

$$s = N \frac{\pi ab}{L^2}. \quad (4)$$

Simulations consider particle numbers from $N = 25$ to $N = 150$, thus covering surface fractions from $s = 3.93\%$ to $s = 23.56\%$.

The second relevant parameter compares the typical kinetic energy K of an SPP and the dipolar interaction potential U in a simple system of two SPP, which depends on the dipole strength. The dimensionless control parameter is

$$\Gamma = \frac{U}{K} = \frac{|U(2a)|}{\frac{1}{2}m\langle v^2 \rangle} \quad (5)$$

with

$$\langle v^2 \rangle = \langle v_a \rangle^2 + \sigma_a^2 + \langle v_b \rangle^2 + \sigma_b^2, \quad (6)$$

where the distance r_{ij} between two dipoles in Eq. (3) is equal to one SPP length $2a$ as long as this parameter was defined considering that the two SPP are one behind another. In the context of these numerical simulations, the mass m is typically 2 g. The terms in Eq. (6) are the parameters of the velocity distributions along the basis axes of a particle (see Table I in the Supplemental Material [32]). We expect that low $\Gamma < 1$ values would imply disordered systems while high $\Gamma > 1$ values would induce particle alignment due to the dipolar magnetic interactions.

III. RESULTS

A. Dynamics with dipolar interactions

Figure 2 presents typical snapshots of $m1a$ systems when both control parameters N and Γ are modified.

As expected, systems remain disordered for low dipolar interactions while structures emerge when high Γ values are

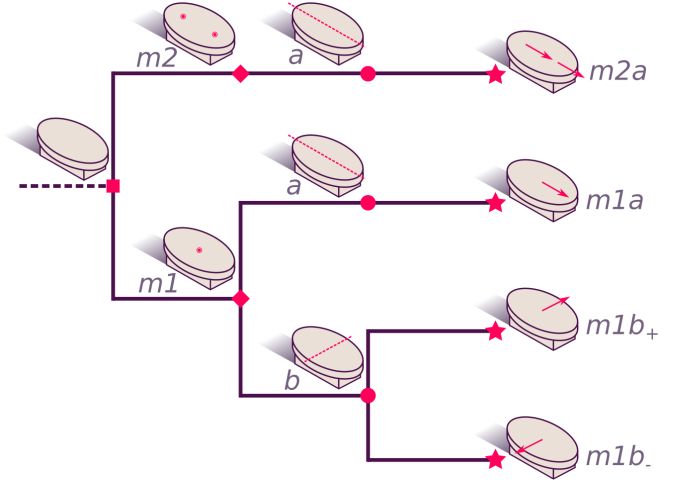


FIG. 1. Phylogeneticlike tree of the different active particles considered in this work. Particles are elliptic vibrobots favorably moving along their long axis a . In those particles, one (noted $m1$) or two (noted $m2$) magnets can be inserted. Magnetic dipoles can be oriented along the major axis (labeled a) or along the minor axis (labeled b), and in this last case, the dipole can be directed towards the left (b_+) or the right (b_-) side of the particle.

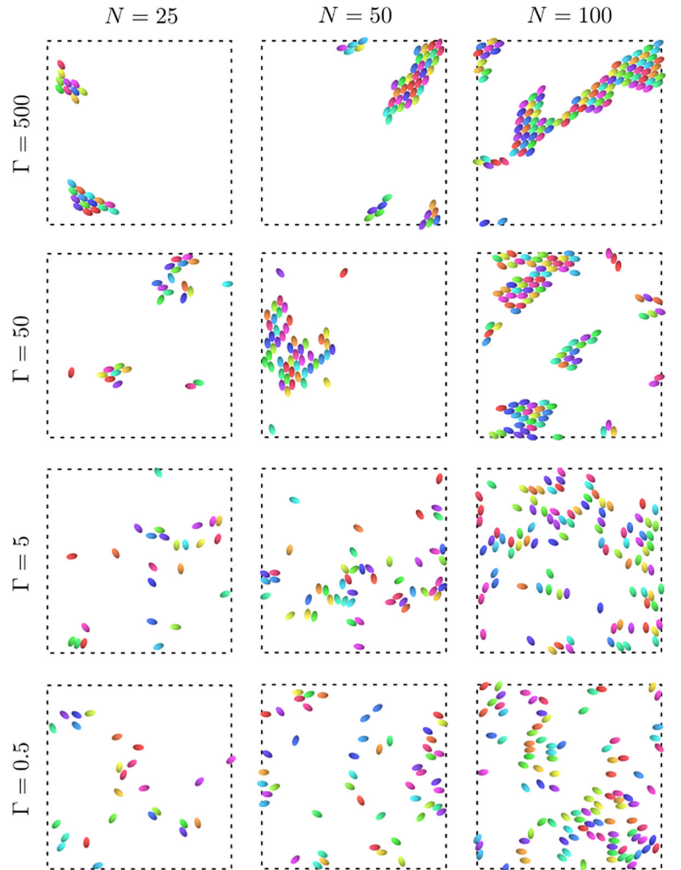


FIG. 2. Snapshots of $m1a$ systems with increasing Γ (from bottom to top) and N (from left to right). We see that collective dynamics are more deeply impacted by increasing dipolar magnetic interactions in comparison with the influence of density.

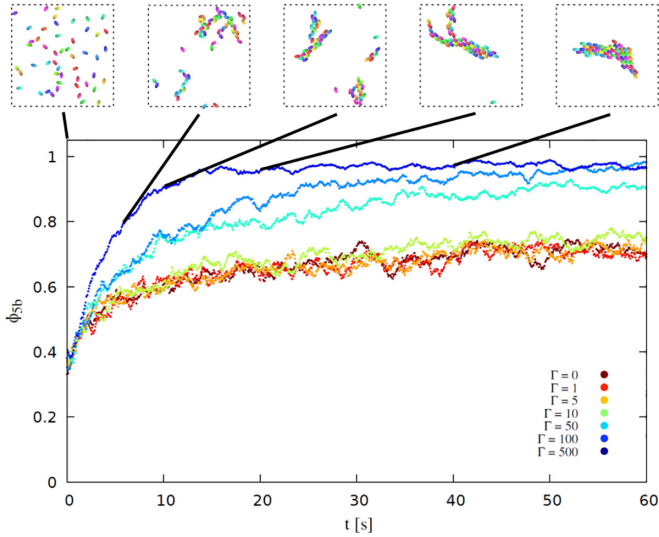


FIG. 3. Time dependence of the local polarization parameter ϕ_{5b} . Each curve is an average over 10 simulations for systems with 50 $m1a$ particles at variable Γ . When Γ is close to zero, the system mainly aligns itself through steric interactions. As the value of Γ increases, so does the intensity of the dipolar magnetic interactions, resulting in an increase of the local polarization and a faster emergence of compact structures. On top of the graph, some snapshots represent the evolution of the system when $N = 50$ and $\Gamma = 500$.

reached. More interestingly, structures appear even for low N values, meaning that they are mostly due to dipolar interactions instead of steric ones.

B. Local polarization

Observations made in Fig. 2 should be completed by a deeper analysis of the local structure. In most numerical studies, the order parameter ϕ , representing the polarization of the system, is considered when SPP are aligning. It is defined as

$$\phi(t) = \frac{1}{N} \left| \sum_{i=1}^N \vec{e}_{a,i}(t) \right|, \quad (7)$$

where the polarization measurement returns zero for a fully disordered system and one if all the particles are perfectly aligned.

In this paper we will use a local parameter that considers the close environment of each particle, within a radius of $5b$. We note ϕ_{5b} the average value of the local alignment over all the particles in the system. Figure 3 presents ϕ_{5b} over simulation time t for different interaction strengths, i.e., for different Γ values. Systems are composed of 50 $m1a$ SPP, corresponding to the central column of Fig. 2. The local polarization increases with time, meaning that SPP are aligning due to their interactions and they eventually form groups which will be analyzed below. At $\Gamma = 0$, when only steric interactions occur in the system, we see a weak increase of the local polarization that remains around $\phi_{5b} \simeq 0.7$ at the end of the simulations. Since this value differs from the initial $\phi_{5b} \simeq 0.35$ for randomly oriented particles, this means that small local crowds emerge as a consequence of the steric interactions. Therefore, this curve is a reference behavior for

dynamics only governed by collisions. We observe that this behavior also appears for low Γ values, meaning that magnetic interactions are not strong enough yet to overcome the natural movement of the particles. However, as Γ increases, so does the intensity of the dipolar magnetic interactions, and such systems exhibit structures in a smaller time window and reach a higher local polarization, typically with $\phi_{5b} \geq 0.85$, even though every system started with a similar random distribution for the initial orientation of the SPP. This means that magnetic interactions first act mainly in the emergence of collective dynamics before being helped by collisions to enhance order in the system. Short-range interactions are therefore able to create structures. We should also notice that even for high Γ values, systems still struggle to reach a steady state after a long time. In particular, all SPP are not perfectly aligned due to the angular movement produced by their self-propulsion.

C. Structures and local order

Simulations show various patterns following the imposed orientation of the dipoles in their SPP and the values attributed to the different control parameters. Figure 4 presents typical behaviors for the three types of SPP. The left column shows some snapshots with different patterns while the right column gives corresponding polar graphs that summarize how particles are relatively positioned by focusing on their immediate environment. To plot the polar graphs, we have compiled each frame of a simulation between 25 and 40 seconds, i.e., the time window during which we assume the system is in a steady state according to Fig. 3. In the polar graphs, a dot indicates the relative position of another particle within a radius of $5b$, with a color that depends on the scalar product between the orientations of both particles, from red for antialigned particles to blue for fully aligned particles. All particles from all the analyzed frames are treated to create the polar graph, where the resulting particle in the center is considered moving in the direction indicated by the black arrow. The red arrows illustrate how the dipoles are placed in the particles.

The top row of Fig. 4 concerns a $m2a$ system that develops vortex dynamics. We see that the main peaks appear in the front and behind the particles. This means that chainlike structures appear. It seems that those chains are flexible and they eventually form loops and vortices. Many scattered red dots suggest that several chains can move close to each other and in opposite directions. In contrast, some localized yellow and orange dots are more typical of vorticing structures. The central row shows a typical pattern formed with a $m1a$ system, with compact groups composed of ordered particles. The corresponding polar graph indeed highlights several more precise peaks in the front and at the back of the particles but also in the close neighborhood. A crystallike structure reminiscent of a hexagonal lattice is observed. The last row shows the typical pattern observed with $m1b$ particles. The dipoles are perpendicular to the major motion of the SPP and strips are observed. The polar graph evidences the strips since peaks are only seen in the direction of the minor axis.

Since the neighborhood is deeply affected by particle type and dipole strength, an additional parameter C is calculated. This parameter is a local coordination number that reports

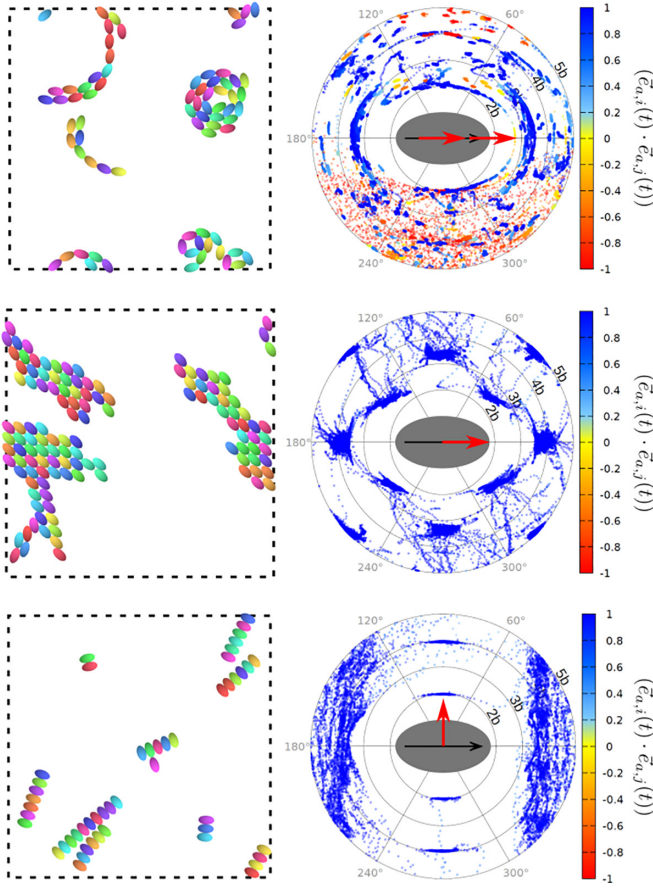


FIG. 4. From top to bottom, results with chains and vortices ($m2a$ -inclusion), flocks ($m1a$ -inclusion), and strips ($m1b$ -inclusion). (left) Representative snapshots of the observed structures. (right) Typical polar graphs show the relative positions and alignments between particles in their close environment (up to distances $5b$). The color scale represents the scalar product between the orientations of each pairwise particle. It ranges from -1 in red for two antialigned particles to one in blue for fully aligned particles. The black arrow represents the direction of motion and the red one represents the dipole inclusions.

the close environment of the particles defined as the average number of neighbors with which a particle is in contact.

IV. DISCUSSION

Since the dipole orientation in the SPP leads to various patterns, the results will be independently discussed for each SPP type as a function of the control parameters. For this purpose, the discussion focuses on two color diagrams, one for each analyzed order parameter, ϕ_{5b} and C , respectively, the average local polarization and the average local coordination number. Averages are performed over the steady state deduced from Fig. 3 and over five independent simulations for each couple (N, Γ) .

A. Chains and vortices

Particles with two dipoles will inevitably provide strong interactions with front and rear particles. The formation of

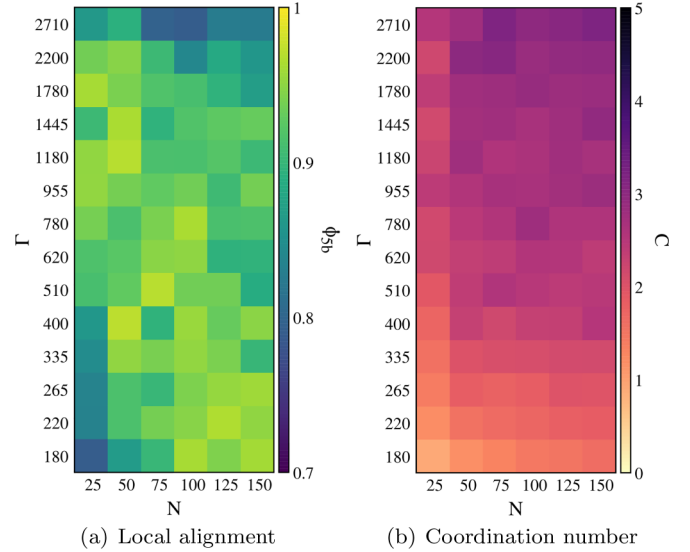


FIG. 5. Order parameters ϕ_{5b} and C for the $m2a$ -inclusion. Three regimes appear on the graphs. When having weak magnetic interactions and low densities ($\Gamma \leq 400$ and $N \leq 75$), SPP have an average of two neighbors, showing that they form *chains*. Because they are quite independent, we observe that the local alignment is not perfect. When the parameters reach high values ($\Gamma \geq 1780$ and $N \geq 75$), SPP gain more neighbors but are still not quite ordered with their close environment, resulting in more *vortices* in the arena. In the intermediate regime, there is a coexistence of phases where both *chains* and *vortices* can be observed at the same time.

chains as seen in Fig. 4 (top row) is therefore not surprising. However, the question is to identify the conditions under which vortices are more likely to form by comparison with simple chains.

Figure 5 shows the color diagrams for the $m2a$ -inclusion. The first remark is the effect of the intensity of the dipolar magnetic interactions. Figure 5(b) exhibits clearly that increasing Γ leads to an aggregation of particles, going from particles with one or two neighbors in contact when $\Gamma \leq 400$, typical of chains structures, to more than two neighbors beyond that value. Looking at the local alignment details the analysis. On one hand, when we have weak magnetic interactions ($\Gamma \leq 400$) and small densities ($N \leq 75$), particles are not close to being fully aligned. Chains are small and quite few in number to have independent trajectories and result in a globally disordered system. On the other hand, when we have strong magnetic interactions ($\Gamma \geq 1780$) and high densities ($N \geq 75$), particles are more connected to each other but are not quite aligned yet. In this case, such systems are mainly composed of compact vortices. In fact, chains are longer and are able to undulate and form loops as detailed in Fig. 6. In the intermediate regime, particles are usually locally aligned and both chains and vortices may coexist in the system. However, chains seem more numerous and the observed vortices are less compact structures in this case.

B. Flocks

When particles have only one dipole orientated to their front, we expect the formation of flocks as seen in Fig. 4 (central row).

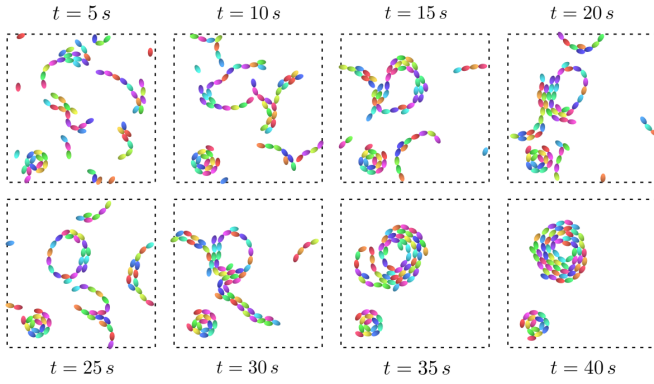


FIG. 6. Detailed evolution of a system with chains and vortices ($N = 75$ and $\Gamma = 400$ for the $m2a$ -inclusion). Snapshots are taken every five seconds and show how long chains progressively undulate and assemble to form large vortices.

Comparing the corresponding color diagrams exposed in Fig. 7 shows that the system faces some difficulties to form stable global structures only in the case of low density ($N < 50$) and weak magnetic interactions ($\Gamma < 180$). No significant order appears because particles are more likely to form several small moving entities that have independent trajectories and little influence on each other. Otherwise, a higher density and/or stronger magnetic interactions allow the system to self-organize. In particular, the density helps the system to have a perfect local alignment while the magnetic interactions also help those emergent structures to be more compact, increasing the average number of neighbors in contact to four or more when experiencing extreme conditions. At the steady state, such systems often display a unique large flock after some collisions between smaller flocks during the simulation, as represented by the inset snapshots in Fig. 3.

C. Strips

As seen in Fig. 4 (bottom row), particles with one dipole orientated to their side will provide strong interactions with

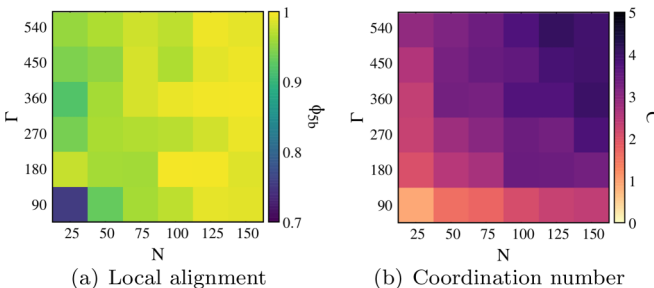


FIG. 7. Order parameters ϕ_{5b} and C for the $m1a$ -inclusion. When the density is low and the magnetic interactions are weak ($N < 50$ and $\Gamma < 180$); the system is globally disordered. SPP assemble into small *flocks* but these emerging structures have no sufficient influence on each other to expect collective dynamics at a large scale. In other cases, increasing one of the control parameters is sufficient to enhance interactions between SPP, which often leads to a unique stable *flock* where SPP have on average four neighbors or more.

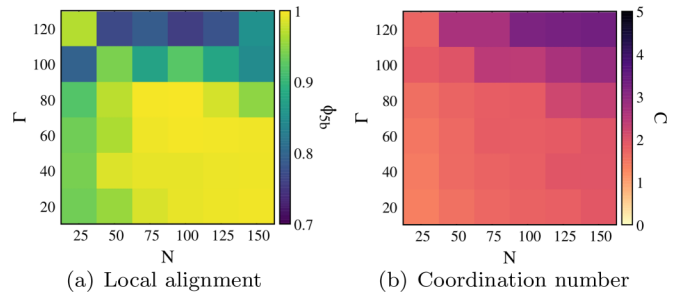


FIG. 8. Order parameters ϕ_{5b} and C for the $m1b$ -inclusion. Three regimes appear on the graphs. In most cases, typically $N \geq 75$ with $\Gamma \leq 80$, the system is fully aligned and has an average of two neighbors, forming *strips*. Their number and length are sufficient to have enough collisions and magnetic interactions with each other which lead to a global alignment. However, if the density is low enough, the average of two neighbors shows that there is also a formation of *strips* but their length and number are too small to have sufficient interactions, decreasing the probability to observe a complete alignment. In the same way, if Γ is high, magnetic interactions are sufficient to create some *layers*, with strips moving in close proximity, one behind another. This configuration occasionally involves different entities facing each other and decreasing the average local alignment.

other particles on their left and right sides, leading to the formation of strips.

On the color diagrams exposed in Fig. 8, three main regimes can be distinguished. In most cases, when the system has a sufficient density ($N \geq 75$) but no quite strong dipolar magnetic interactions ($\Gamma \leq 80$), the emerging strips are large and influence each other. This leads to a global collective motion in the same direction even if each individual strip has its own independence and does not assemble with one another once formed. We see on the diagram that particles are almost fully aligned and have on average two neighbors, one on each side. With a low-density system ($N \leq 50$), the situation is similar to flocks with weak interactions. Several small strips appear but their limited number allows them to have independent trajectories. Each particle also has two neighbors on average, but that behavior reduces the local alignment. In a similar way, if the system has strong dipolar magnetic interactions ($\Gamma \geq 100$), the attraction between particles is high enough to assemble several strips in layers, a more compact agglomeration of particles. These flocklike patterns are indicated by the higher coordination number, with particles that have three or four neighbors. The polar graph in Fig. 4 (bottom row) highlights what happens with different peaks in front of and behind the particles. However, the shape of such structures leads to situations where two strips or layers moving in opposite directions fit into each other. The resulting structure moves at a lower speed and its composition decreases the average local alignment.

D. Low density patterns

From the above observations of three types of SPP, we can conclude that some collective dynamics are emerging at low densities when the dipole-dipole interaction is strong enough to overcome the intrinsic noise of the particles. Indeed, all phase diagrams show at least one structured regime for a low

number N of SPP. Since the interactions are shortrange, these patterns are building up on the successive collisions between particles. Vortices are forming without wall effects. Therefore, our numerical results suggest that dipolar self-propelled particles are relevant for future experiments, such as exploring new configurations with the dipoles embedded in the particles or adding external dipoles in order to create barriers or traps and studying how active matter behaves in a potential well.

V. CONCLUSION

Social behaviors are as diverse as animal communities in nature, and the model presented in this study is a good way to approach them with a simple system. Though, including dipolar magnetic interactions is the only feature that distinguishes this model from the basic ones in the research field of active matter. Various patterns are observed—such as chains, vortices, flocks, and strips—depending on the way the dipoles are inserted in the self-propelled particles, but these dynamics can also be diversified with the control of the intensity of the magnetic interactions. We showed that reinforcing attraction and repulsion between particles helps the system to rapidly reach a steady state and to exhibit collective dynamics while

collisions continue to play a role in the global order in the system after the main structures have been formed. In addition, systems do not need a large number of particles to be able to organize themselves. However, dynamics vary depending on a subtle control of both the density and intensity of the magnetic interactions.

We also showed that behaviors are only dependent on the interactions between particles because the imposed periodic boundary conditions exclude any interactions with walls, corners, or obstacles. This remark is especially relevant for vortices formation.

This study focused on three configurations of dipoles inserted in particles but many other configurations remain to be explored and constitute a large perspective for this work, as well as the reproduction of those systems in an experimental way.

ACKNOWLEDGMENTS

This work is financially supported by the University of Liège through the CESAM Research Unit. N. Vanesse is financially supported by FRS-FNRS (Brussels, Belgium) through Grant No. PDR.T.0251.20.

-
- [1] C. Becco, N. Vandewalle, J. Delcourt, and P. Poncin, Experimental evidences of a structural and dynamical transition in fish school, *Physica A* **367**, 487 (2006).
 - [2] K. Faucher, E. Parmentier, C. Becco, N. Vandewalle, and P. Vandewalle, Fish lateral system is required for accurate control of shoaling behaviour, *Anim. Behav.* **79**, 679 (2010).
 - [3] N. Miller and R. Gerlai, From schooling to shoaling: Patterns of collective motion in sebrafish (*Danio rerio*), *PLoS ONE* **7**, e48865 (2012).
 - [4] D. S. Calovi, U. Lopez, S. Ngo, C. Sire, H. Chaté, and G. Theraulaz, Swarming, schooling, milling: Phase diagram of a data-driven fish school model, *New J. Phys.* **16**, 015026 (2014).
 - [5] M. Nagy, Z. Ákos, D. Biro, and T. Vicsek, Hierarchical group dynamics in pigeon flocks, *Nature (London)* **464**, 890 (2010).
 - [6] R. F. Storms, C. Carere, F. Zoratto, and C. K. Hemelrijk, Complex patterns of collective escape in starling flocks under predation, *Behav. Eco. Soc.* **73**, 10 (2019).
 - [7] M. Ballerini *et al.*, Empirical investigation of starling flocks: A benchmark study in collective animal behavior, *Anim. Behav.* **76**, 201 (2008).
 - [8] A. Attanasi *et al.*, Emergence of collective changes in travel direction of starling flocks from individual birds' fluctuations, *J. R. Soc. Interface.* **12**, 20150319 (2015).
 - [9] B. Zhang, A. Sokolov, and A. Snezhko, Reconfigurable emergent patterns in active chiral fluids, *Nat. Commun.* **11**, 4401 (2020).
 - [10] A. Nourhani and D. Saintillan, Spontaneous directional flow of active magnetic particles, *Phys. Rev. E* **103**, L040601 (2021).
 - [11] J. R. Howse, R. A. L. Jones, A. J. Ryan, T. Gough, R. Vafabakhsh, and R. Golestanian, Self-Motile Colloidal Particles: From Directed Propulsion to Random Walk, *Phys. Rev. Lett.* **99**, 048102 (2007).
 - [12] H. Zhao, H. Liu, Y.-W. Leung, and X. Chu, Self-adaptative collective motion of swarm robots, *IEEE Trans. Automat. Sci. Eng.* **15**, 1533 (2018).
 - [13] G. Wang *et al.*, Emergent Field-Driven Robot Swarm States, *Phys. Rev. Lett.* **126**, 108002 (2021).
 - [14] T. Vicsek, A. Czirók, E. Ben-Jacob, I. Cohen, and O. Shochet, Novel Type of Phase Transition in a System of Self-Driven Particles, *Phys. Rev. Lett.* **75**, 1226 (1995).
 - [15] I. D. Couzin, J. Krause, R. James, G. D. Ruxton, and N. R. Franks, Collective memory and spatial sorting in animal groups, *J. Theor. Biol.* **218**, 1 (2002).
 - [16] D. Grossman, I. S. Aranson, and E. Ben-Jacob, Emergence of agent swarm migration and vortex formation through inelastic collisions, *New J. Phys.* **10**, 023036 (2008).
 - [17] C. K. Hemelrijk and J. Wantia, Individual variation by self-organisation, *Neurosc. Bio. Rev.* **29**, 125 (2005).
 - [18] P. K. Ghosh, V. R. Misko, F. Marchesoni, and F. Nori, Self-Propelled Janus Particles in a Ratchet: Numerical Simulations, *Phys. Rev. Lett.* **110**, 268301 (2013).
 - [19] V. Telezki and S. Klumpp, Simulations of structure formation by confined dipolar active particles, *Soft Matter* **16**, 10537 (2020).
 - [20] T. Vicsek and A. Zafeiris, Collective motion, *Phys. Rep.* **517**, 71 (2012).
 - [21] J. Delcourt, N. W. F. Bode, and M. Denoël, Collective vortex behaviors: Diversity, proximate, and ultimate causes of circular animal group movements, *Quart. Rev. Bio.* **91**, 1 (2016).
 - [22] S. Bazazi, K. S. Pfenning, N. O. Handegard, and I. D. Couzin, Vortex formation and foraging in polyphenic spadefoot toad tadpoles, *Behav. Ecol. Sociobiol.* **66**, 879 (2012).
 - [23] M. Rubenstein, C. Ahler, N. Hoff, A. Cabrera, and R. Nagpal, Kilobot: A low cost robot with scalable operations designed for collective behaviors, *Robot. Auton. Syst.* **62**, 966 (2014).

- [24] P. Baconnier, D. Shohat, C. Hernández López, C. Coulais, V. Démery, G. Düring, and O. Dauchot, Selective and collective actuation in active solids, *Nat. Phys.* **18**, 1234 (2022).
- [25] E. Altshuler, J. M. Pastor, A. Garcimartín, I. Zuriguel, D. Maza, and C. M. Aegerter, Vibrot, a simple device for the conversion of vibration into rotation mediated by friction: Preliminary evaluation, *PLoS One* **8**, e67838 (2013).
- [26] J. Deseigne, O. Dauchot, and H. Chaté, Collective Motion of Vibrated Polar Disks, *Phys. Rev. Lett.* **105**, 098001 (2010).
- [27] C. A. Weber, T. Hanke, J. Deseigne, S. Léonard, O. Dauchot, E. Frey, and H. Chaté, Long-Range Ordering of Vibrated Polar Disks, *Phys. Rev. Lett.* **110**, 208001 (2013).
- [28] J. Deseigne, S. Léonard, O. Dauchot, and H. Chaté, Vibrated polar disks: Spontaneous motion, binary collisions, and collective dynamics, *Soft Matter* **8**, 5629 (2012).
- [29] N. H. P. Nguyen, D. Klotsa, M. Engel, and S. C. Glotzer, Emergent Collective Phenomena in a Mixture of Hard Shapes Through Active Rotation, *Phys. Rev. Lett.* **112**, 075701 (2014).
- [30] K. Yeo, E. Lushi, P. M. Vlahovska, Collective Dynamics in a Binary Mixture of Hydrodynamically Coupled Microrotors, *Phys. Rev. Lett.* **114**, 188301 (2015).
- [31] C. Scholz, M. Engel, and T. Pöschel, Rotating robots move collectively and self-organize, *Nat. Commun.* **9**, 931 (2018).
- [32] See Supplemental Material at <http://link.aps.org/supplemental/10.1103/PhysRevE.108.024608> for details of the DEM model with parameter values and implementation of interaction forces.
- [33] P. A. Cundall and O. D. L. Strack, A discrete numerical model for granular assemblies, *Géotechnique* **29**, 47 (1979).